American Journal of Science, Engineering and Technology
2016; 1(2): 27-41
http://www.sciencepublishinggroup.com/j/ajset
doi: 10.11648/j.ajset.20160102.13

Decentralized Control of Low-Voltage Islanded DC Microgrid Using Power Management Strategies

Mehrdad Beykverdi[1], Abolfazl Jalilvand[2], Mehdi Ehsan[3]

[1]Department of Electrical Engineering, Science and Research Branch, Islamic Azad University, Tehran, Iran

[2]Department of Electrical Engineering, University of Zanjan, Zanjan, Iran

[3]Department of Electrical Engineering, Sharif University of Technology, Tehran, Iran

Email address:

ajalilvand@znu.ac.ir (A. Jalilvand)

To cite this article:

Mehrdad Beykverdi, Abolfazl Jalilvand, Mehdi Ehsan. Decentralized Control of Low-Voltage Islanded DC Microgrid Using Power Management Strategies. *American Journal of Science, Engineering and Technology.* Vol. 1, No. 2, 2016, pp. 27-41.
doi: 10.11648/j.ajset.20160102.13

Received: November 6, 2016; **Accepted**: December 9, 2016; **Published**: January 5, 2017

Abstract: This paper intended to control a DC microgrid in islanded operation mode using decentralized power management strategies. The DC microgrid under study included a wind turbine generator (WTG), photovoltaic (PV), battery energy storage system (BESS) and dc constant power load. According to the newly proposed strategy, each of distributed generation sources of energy and battery energy storage system can be deployed independently within any controlled microgrid through the droop method. Proposed I/V characteristic curve could be regulated locally and in real-time based on the available power of DGs and the battery state of charge (SOC), to synchronize the module performances independently and establish the power balance in the DC microgrid. Proposed strategy for the battery enables the system to supply independently the power required for the load demand when the DGs are not capable of supplying the required power to the load. This can maintain the common bus voltage within the allowable range and establish the power balance in the DC microgrid. The proposed control strategy was applied locally and without dependency on telecommunication links or any centralized energy management system on each of the distributed generation modules and battery independently. The newly proposed power management strategy was simulated through the implementation of a low voltage DC microgrid in MATLAB/SIMULINK where its performance was evaluated.

Keywords: DC Microgrid, Distributed Generations, Energy Storage, Islanded Operation, Droop Control

1. Introduction

In recent decades, the ever-increasing utilization of energy distributed generation systems has led to growingly extensive research efforts in this area. The prospect of generating electricity from clean energy sources and local power generation near consumers has fundamentally revolutionized the approach to traditional centralized power systems and large-scale production. Electrical systems developed from small-scale distributed energy resources such as wind turbines, fuel cells, photovoltaic cells, energy storage devices, etc. can be used separately or connected to a network. Many of these sources of energy directly yield DC or AC variable voltage/frequency outputs [1]-[4].

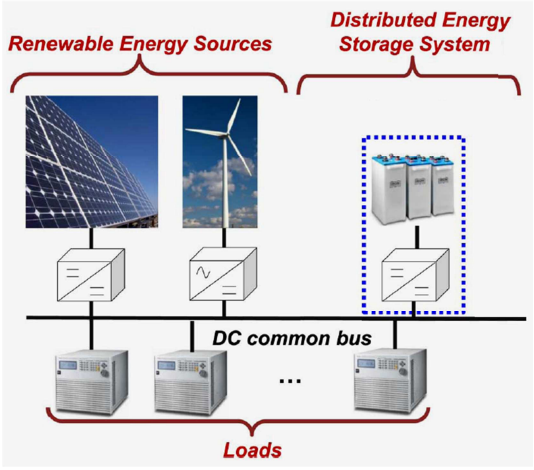

Figure 1. *Structure of islanded DC microgrid.*

Microgrid refers to a set of Distributed Generation (DG) sources, control systems and loads that can independently supply the power required for the consumers in secure condition with high reliability. Hence, the power electronics technologies play a vital role in the structure of a microgrid. Local control system in a microgrid must be designed so as to fulfill the stability of the microgrid under critical situations and errors such as reduce level of power generation (due to intermittent nature of DGs), upstream network outages, short-circuit in the feeder, etc., as well as to prevent any consumers power supply cut-off [5]-[6].

When the DC microgrid is controlled in a centralized procedure, the connection point to the distribution network will be where the controller is applied. The DC microgrid central controller simultaneously pursues several important targets such as economic management of the microgrid, load supply at a given voltage level, voltage control, etc. [7]. In this control method, there are additional control levels, including load controllers and DG controllers, among which the central controller manages the operation of the microgrid. Load control plans are mostly in the shape of load shedding while the DG controllers deal with active power control. The islanded structure of a microgrid occurs due to unplanned events such as faults or planned events such as maintenance or repair. It is noteworthy that under islanded conditions, voltage should be controlled through power electronic converters. When the DC microgrid is connected to the distribution network, the converters of distributed generation sources are controlled as V-I, because the distribution network serves as reference voltage and power supply. In the islanded mode where there is no distribution grid connection, such variations are covered by modifying the parameters and optimizing the converter controls [8]-[9]. Generally, there are two techniques to control a DC microgrid in islanded mode: Single Master Operation and Multi Master Operation [10]. In the single master operation, Voltage Source Inverter (VSI) is used to control voltage during outages and monitoring of certain malfunctions in the microgrid performance. The rest of the converters operate as V-I, receiving their settings data from the MicroGrid Central Controller (MGCC). In the multi master operation, the VSI converter functions as a voltage reference and active power. These converters can connect to energy storage sources such as batteries, fly wheels or DGs, to regulate their output active power according to the grid voltage. At the time of voltage deviation, the energy storages stay in active power absorbs or inject mode so as to zero the voltage variations. Due to limited energy of these storage devices, voltage control will be possible though these devices only for a limited period. The V-I converters continue operating as before and central control modifies the specifications, parameters and new operating points, so as to achieve a far better control on the microgrid [11]-[15]. In the decentralized DC microgrid control, the DGs control their coverage area simply based on local measurements. In fact, each source has its own independent or adaptive control, modifying its generation power separately for voltage control. Each controller should meet the following requirements [16]-[17]:

- Capability to load sharing (linear or nonlinear).
- Guarantee the stability of the entire system.
- Converter control should prevent DC voltage offset in the microgrid.

The performance and control of a DC microgrid can be evaluated either in connected or isolated (islanded) condition. The DC microgrid is usually modeled as a combination of wind turbines, batteries, PV arrays, loads and DC voltage source converters. When the microgrid is connected to the upstream distribution system, the active power consumption is supplied through the main network in order to provide stability and maintain the DC bus voltage. When the microgrid is detached from the distribution feeder because of faults or failure to supply load power, the DC loads must be met through a smart strategy adopted to the DGs and battery system, so as to maintain system stability and supply the power requirements [18]-[20]. Hence, the microgrid controllers generally serve to develop a monitoring system with appropriate performance to ensure reliable and safe energy supply for consumers and energy storage system based on measuring the DC bus voltage. Research and development of adaptive control systems aimed at improving the behavior and economic performance of DC microgrid through hierarchical control has been a controversial topic in the field of DC microgrid energy management. The microgrid economic performance in tertiary-level of hierarchical control involves and analysis islanding formation, load recovery and re-synchronization with the main network. The DG outputs are stabilized and delivered to the power electronic converters through internal and external control loops including PI controller. Generally, converters are controlled through Pulse Width Modulation (PWM) based on I/V droop characteristic curve. The microgrid voltage stability and steady state error of controllers are realized at the primary and secondary levels. At the tertiary-level of control, the economic performance of the microgrid can be obtained through a centralized energy management system or through the System Control and Data Acquisition (SCADA) [21]-[22]. One disadvantage of this method involves centralized microgrid control and system dependency on the communication links that decreases the reliability of the system. The utilization of smart systems for droop control and local control of DC microgrids are regarded as efficient methods in this area. The smart decentralized strategy is adopted based on fuzzy logic to achieve power balance in the microgrid aimed at specifying the virtual resistance range for droop controllers in accordance with the status of each DG or the state of charge in each energy storage device [23]. In other words, the allowable resistance range is specified in a microgrid so as to establish the power balance and reduce the deviation of DC common bus voltage. All modules in a decentralized control system are controlled only through local variables locally; as result, the microgrid can operate independently and without telecommunications infrastructure. In addition, the microgrid smart management system can adopt optimization rules so

that the system can exchange the communications data, representing the subsystem performance through the ZigBee network [24]. In order to increase the storing energy level in the microgrid and avoid the load shedding scenario in the microgrid, two or more energy storage systems can be applied as battery or super-capacitor. Moreover, in order to overcome the control challenges involved in synchronization of energy storage sources within a microgrid, a two-layer hierarchical control strategy can be adopted [25]-[26]. To achieve this target, the primarily control layer functions through adaptive voltage-droop aiming to regulate the common bus voltage support the battery charge status close to each other in the process of recharging. The second control layer involves a regulatory measure designed be to use the low bandwidth communications interface between the central controller and DGs, which can collect data needed to calculate the virtual resistors adaptively and control the criterion of microgrid operation mode modification in the first layer. The microgrid operation modes include: The process of charging and discharging batteries, DC common bus voltage and load shedding in case of non-supply of power from distributed generation sources and energy storage systems.

This investigation involved autonomous control strategies for PV module, WTG and battery within a DC microgrid through the droop control method. All distributed generation units and batteries are controlled as voltage sources following the adaptive I/V characteristic curve. The adaptive I/V characteristic curve is regulated locally and in real-time based on the available power of DGs, load demand and battery charge level (SOC), so as to achieve decentralized control and power balance in the microgrid. Depending on the generation and load demand, PV module delivers the power generation to the microgrid based on the MPPT algorithm and WTG as well as the droop curve. Alternatively, it independently stores the excess energy in the battery in the case of total generation power is more than the load demand. In other words, BESS undertakes supplying the load demand only in a mode where the total power load is more than the total generation power of DGs. At this point, the battery system supplies the power load shortage based on the SOC. The control strategies for each module within the microgrid were implemented through multi-loop control without using communication links or central energy management system.

2. DC Microgrid Structure

Application of a DC microgrid can improve stability, reduce losses and enhance the flexibility of the power system. Generally, the microgrids entail several advantages including greater energy efficiency, lower costs of generation and transmission and reduced greenhouse gas emissions. As opposed to the AC microgrids, the DC microgrids inherently entail certain advantages such as simplicity in control system design, since there is no need to control the frequency. Microgrids design and control can decrease the number of stages involved in DC power electronic conversion and curtail the switching losses. Moreover, DC systems will not face challenges such as harmonics and inrush current of power transformer. The advantages of the DC microgrid over the conventional AC microgrids can be categorized as follows [27]-[29]:

1. More than 90% of household loads can be directly fed by the DC power; such as the devices based on microprocessors, PC power supplies, switching power supplies, electronic ballasts for fluorescent lighting, LED lights and variable frequency drives in heating, cooling and ventilation systems.
2. The DC power can maximize the generation power through sources such as photovoltaic and fuel cell in order to prevent the power conversion losses (eliminating one or two stages of power conversion, absence of reactive power and harmonics). In conventional AC systems, the energy generated by PV is converted to AC and is converted again to the DC power in another stage for some consumers.
3. The DC power can effectively adapt with energy storage systems and enhancing the efficiency of the system. Moreover, it is widely applied in hybrid vehicles.
4. A major portion of the distributed generation sources (such as photovoltaic, fuel cells and micro-turbines) are inherently DC sources that can be directly used to enhance energy efficiency and optimize system productivity.
5. By using the existing infrastructure in the available distribution system (e.g. cable structures), the available distribution systems can be utilized as DC network so as to achieve cost savings.
6. There is no need to synchronize the energy generation sources within the DC microgrid.
7. The power fluctuations in the DGs and power loads can be compensated on the DC line by energy storage devices.
8. Loads are not affected by increasing or decreasing voltage, three-phase voltage imbalance or voltage harmonics.
9. Inrush current and single phase generators have no impact on the power quality.

Figure 2 illustrates the block diagram of the DC microgrid under study. In the mentioned figure, the first module is PV, the second module is wind turbine generator (WTG) and the third module is the battery energy storage system (BESS). Furthermore, R represents the feeder resistance. The PV module is connected to DC bus by a DC-DC converter as the droop control strategies are adopted on this converter where the switching is controlled through the PWM method. As mentioned earlier, unlike previous studies, the PV module was controlled as a voltage source, which was one of the innovative aspects of this investigation. Since the WTG has a three-phase AC output, it is first converted by a full-wave rectifier into DC output applied on a DC-DC converter based on droop control strategy. Similar to the PV module, the

battery energy storage system (BESS) is connected to the microgrid common bus by a DC-DC power electronics converter, controlling the battery charging and discharging process. The microgrid load was supposed to be constant power, to evaluate the microgrid control strategies by decreasing or increasing level of load power.

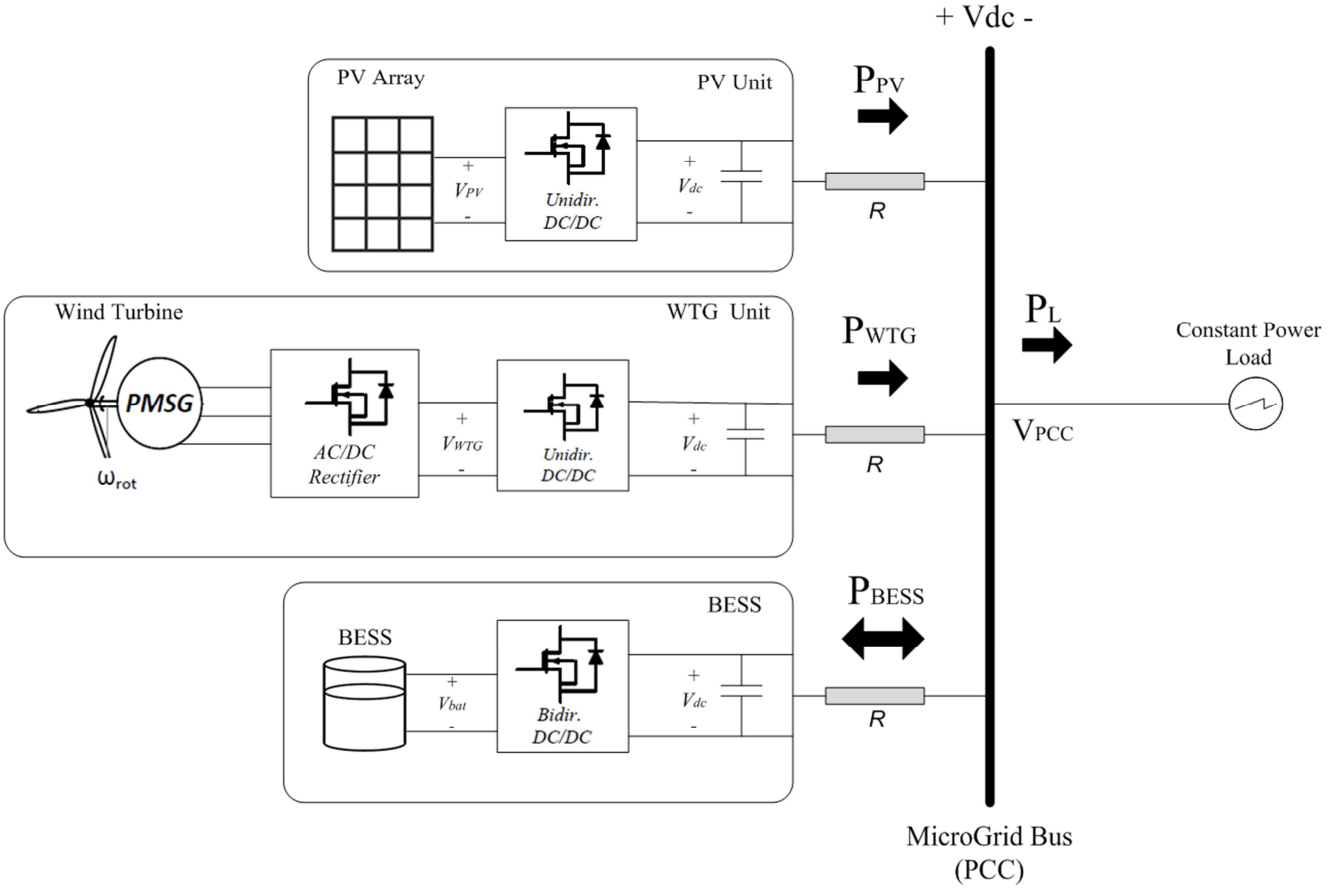

Figure 2. *Block diagram of proposed DC microgrid.*

3. Problem Statement and Objectives

The main focus of this research was on the design of local control strategies for PV module, WTG and battery so as to achieve full decentralized synchronization for power flow within the DC microgrid. The independent control strategies considered for the above modules have several functional features including:

3.1. PV and WTG

The PV and WTG modules were supposed to be able to deliver their total power generation to the DC microgrid whenever there was load demand. The priority of power delivery was upon the PV module. In the case of load demand exceeded the maximum power generated by PV, WTG would supply the rest of required power based on its droop characteristic. The PV and WTG units must be able to adapt their output power to the load demand by independent control strategy in real-time. If there is excess power, they are supposed to deliver their energy surplus to the battery until maximum battery SOC has been fulfilled. Changing the condition of power delivery between PV and WTG as well as output power control of units should be achieved through local control strategy without depending on any external reference signal, communication links or a centralized energy management system.

3.2. Battery Unit

The battery unit will supply power only when the total load demand exceeds the power generation of DGs in the microgrid. In other words, the battery will be used to meet peak load. In other situations, however, the battery will remain in charging or floating mode. The power required to recharge the battery will be specified based on load demand, total power generation and battery SOC so as to establish the power balance in the DC microgrid. Similar to the distributed generation units, the battery will be able to switch modes from charging to load power supply without any need to communication links or a centralized energy management system. Hence, the battery status will be changed and charge level will be determined by the local controllers independently.

In this paper, all of the above objectives were fulfilled by local control over the distributed generation units and the battery as a voltage source following the adaptive I/V characteristic curve. According to the proposed I/V characteristic, depending on the production level or power

consumption at any moment, one of the PV, WTG or battery is responsible for regulating the DC microgrid common bus voltage so as to prevent the voltage exceeds from the allowable limit, while the other units contribute as controlled power sources. Toggling modes between voltage regulation and power regulation will be realized independently by applying the adaptive I/V characteristic curve within the local controllers.

4. Distributed Generations Control Strategy (PV and WTG)

The decentralized power management of PV and WTG as well as the battery system is realized through interaction between the proposed I/V characteristic curve and droop characteristic of PV and wind turbine (all modules were assumed to act as a voltage source). The DC-DC converter in PV module serves to deliver the total power available in the unit to the microgrid through the DC link voltage monitoring with a nominal value of $V_{dc\text{-}ref}$. In other words, the DC-DC converter injects the PV module power into the DC link by regulating the voltage in DG terminal. According to Figure 3, the PV module output voltage is applied to control the power delivered to the microgrid as the PI controller adjusts its output power based on voltage deviations. Additionally, the maximum power of PV module is traced delivered through the MPPT algorithm based on Perturb & Observe method, which will be explored in the results of simulation.

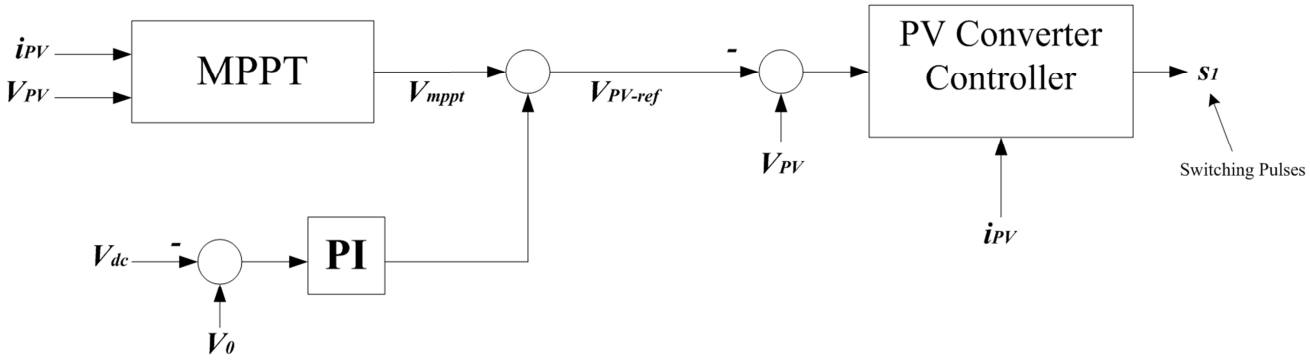

Figure 3. *PV DC-DC converter controller.*

As previously mentioned, increase or decrease in the power generation of PV (power change in the MPPT algorithm or decrease/increase in solar radiation level) transfers I/V characteristic to the right or left, respectively. Figure 4 displays the synchronization of power flow in the DC microgrid in response to power variations of PV module. According to this figure, if the output current of the module increases from point $I_{pv\text{-}mppt\text{-}A}$ to $I_{pv\text{-}mppt\text{-}B}$, the I/V characteristic curve will be transferred to the right, thus curtailing the current delivered to the wind turbine from $I_{WTG\text{-}A}$ to $I_{WTG\text{-}B}$. This change increases the voltage from V_A to V_B due to reduced power delivery of WTG based on its droop characteristic. Moreover, if the PV module power generation exceeds the load demand ($I_{pv\text{-}mppt}>I_L$), then the wind turbine power generation will become zero and PV module acts as a controlled power source and will supply the load demand.

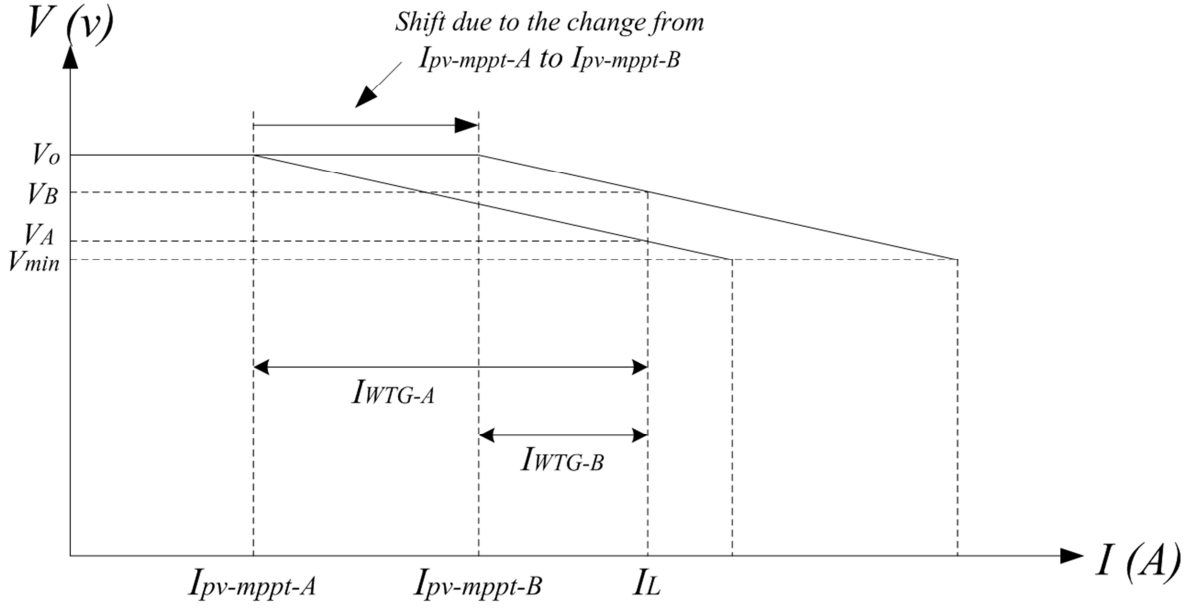

Figure 4. *I/V characteristic of PV unit and MPPT changing from point A to B.*

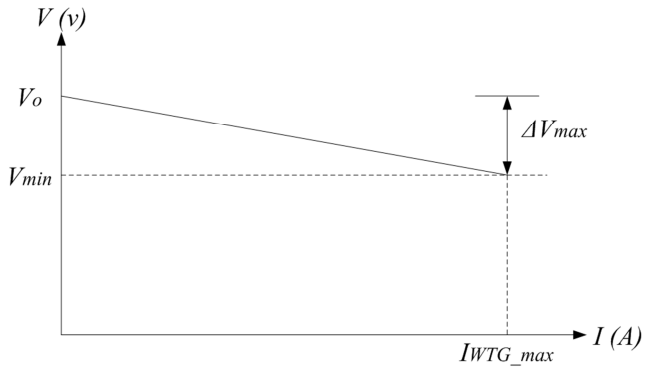

Figure 5. *I/V characteristic of WTG unit.*

Figure 5 shows I/V characteristic curve for WTG. According to the proposed droop curve, the wind turbine is assumed to act as a voltage source following the corresponding characteristic. In order to simplify and put into practice the control scheme, the dynamics of the wind turbine were disregarded. In the mentioned figure, V_0 represents the nominal DC link voltage in the network, V_{min} is the minimum voltage of DC bus, and $I_{WTG-max}$ is the wind turbine maximum current generation which can be injected into the DC microgrid. It is worth noting that the droop slope of WTG was equal to the virtual resistance droop (R_d) of the WTG control unit.

Figure 6 shows the block diagram of WTG droop control. According to this diagram, the PI controllers reduce the measurement error at any moment through sampling of voltage and current output of DC-DC converter, applying droop resistance and generating the reference voltage and current values, which will be eventually controlled through the PWM converter control unit. Regardless of the microgrid voltage regulated by WTG within the range of V_0 and V_{min}, the PV module stabilizes its power output on the $P_{PV-MPPT}$ value that changing the droop curve in WTG.

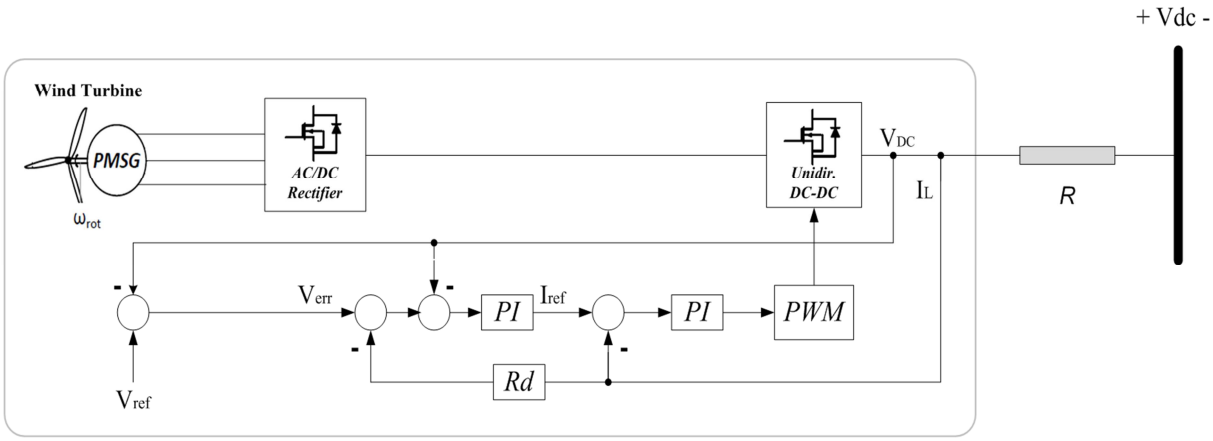

Figure 6. *Droop control diagram of WTG unit.*

The I/V characteristic curve of PV and WTG can be combined into a single curve, which describes the PV module performance in a microgrid controlled through droop as shown in Figure 7. It is noteworthy that change in load demand leads to variation of I/V characteristic curve operating point from A to B or C, while a change in PV power generation would shift the entire I/V curve to the right or left.

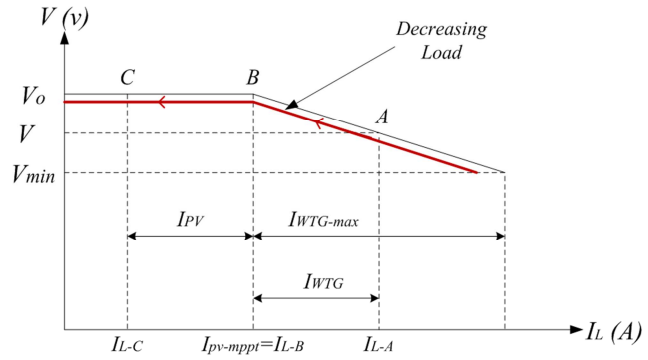

Figure 7. *Equivalent I/V characteristics of DGs in DC microgrid.*

According to droop characteristic above, the DC microgrid behavior in response to the load demand (power consumption variation) and DG production conditions can be described through the following scenarios:

1. $I_{PV-MPPT} \leq I_L \leq (I_{PV-MPPT}+I_{WTG-max})$: In this scenario, the PV module delivers its maximum power in accordance with MPPT algorithm, while the rest of load demand is supplied by the WTG. This operating point has been marked as I_{L-A} in Figure 7. Notably, the microgrid voltage is regulated by the DGs based on the droop curve of each module. In other words, each of the distributed generation units distribute the power generation according to its droop characteristic.
2. $I_{PV-MPPT} > I_L$: Based on the droop curve, the WTG increases the microgrid common bus voltage in response to reduced load demand. By reducing the load demand, the microgrid voltage increases until the entire load is supplied by the PV module at point B, $V=V_0$ shown in Figure 7. Hence, any reduction in load demand will force the WTG to increase the voltage more than V_0 based on its droop characteristic. In this case, the total load demand is supplied by the PV

module as the power output of WTG becomes zero (point I_{L-C}). Since the voltage increase is not allowed to exceed V_0, the PI controller in Figure 3 adjusts the voltage limitation within V_{dc-ref}, to make zero the voltage error. In this mode, the PV controller transfers the operating point out of the MPP region, regulating the PV power generation proportionate to the load demand. Moreover in this case, if the load demand begins to increase once again, the DC link voltage tends to decrease below V_{dc-ref}. As a result, the MPPT algorithm is re-activated and regulates the PV operating point on the MPP region until the maximum power is delivered to the load demand. Since the microgrid voltage will begin to decrease, if the load demand exceeds $I_{PV-MPPT}$, the WTG begins to deliver the power in accordance with its droop characteristic, supplying a portion of the power not supplied by the PV module.

3. $I_{PV-MPPT}$ variations: As mentioned earlier, changes in the PV power generation leads to a shift in microgrid I/V characteristic curve to the right or left. In fact, as shown in Figure 7, if the PV travels from its ordinary operating point to MPP, the above curve will be shifted to the right. In this mode, WTG power generation sharing will decrease because of the increase in PV generation. Therefore, the microgrid voltage increases to the reference voltage V_0 due to reduced power generation of WTG controlled by droop method. In this scenario, if the PV generation power is greater than the maximum load demand, the share of WTG generation power will become zero as the PV transfers its operating points out of the MPP region, stabilizing the microgrid voltage limitation within the reference values similar to a voltage source.

5. Battery Control Strategy

This section elaborates on the control diagram and droop characteristic of battery control unit. The battery DC-DC converter is controlled to adjust the output current in $-I_{ch-ref}$ by regulating the output voltage. The current $-I_{ch-Ref}$ represents the reference battery charge current varying within the range of zero to I_{ch-max} based on SOC and the structural properties of the battery. Furthermore, the voltage amplitude will vary in the range of V_0 and V_{min} based on the battery control system within the specified charging current. It is noteworthy that reference current I_{ch-ref} can be specified based on the battery SOC using a fixed charging curve [30]-[33]. Moreover, I_{ch-ref} could be produced based on battery voltage through two or three-stage charging scenarios [34]. Notably, since the main focus of this research is on the development of DC microgrid energy management strategies, it was suitable to involve a similar reference charging curve [32] for this purpose. The battery charging curve has been shown in Figure 7, where the exponential section was calculated by Equation (1):

$$I_{ch-ref} = I_{B-max} - I_{B-max}\left(1 - e^{-\frac{SOC - SOC_{ref} + \delta SOC}{\delta SOC / k_\delta}}\right) \quad (1)$$

In the above equation, SOC_{ref} represents the reference battery charge level to which the controller of the BESS tends to reach to this SOC level. When the battery charge level reaches SOC_{ref}, the constant K_δ will determine how fast the reference charge current I_{ch-ref} approaches to the zero (i.e. battery discharge rate). Both K_δ and δSOC are selected according to structural specifications and design preference of battery.

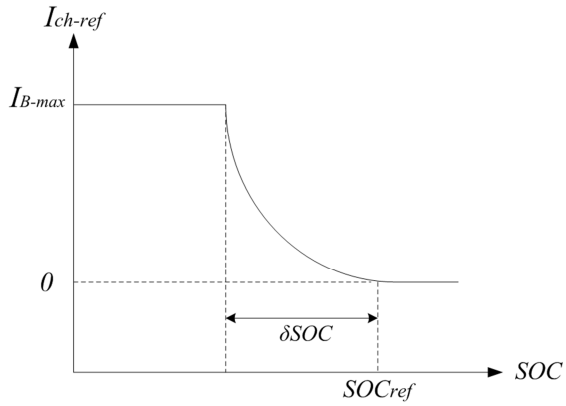

Figure 8. *I_{ch-ref}/SOC charging curve.*

The I/V characteristic curve for Wind Turbine Generator (WTG) and the battery can be combined into a single curve capable of displaying the DC microgrid performance without taking into account the dynamics of PV module as in Figure 9.

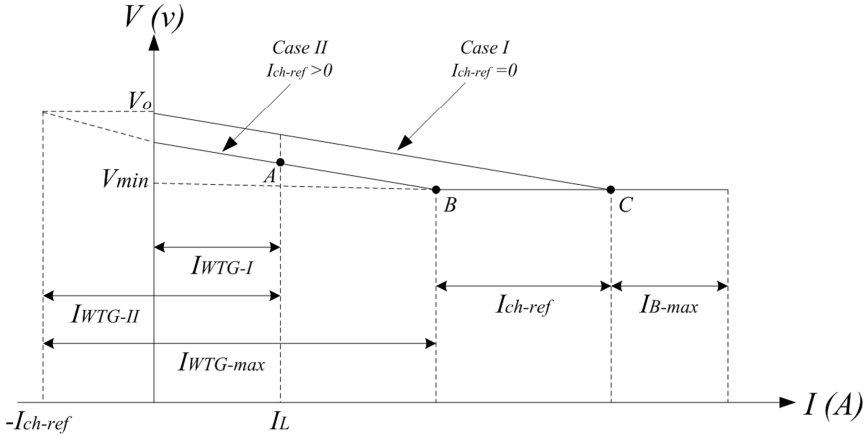

Figure 9. *Equivalent I/V characteristics curve of WTG and battery for different I_{ch-ref} values.*

Case I displays I/V curve in a mode where the battery is fully charged, $I_{ch\text{-}ref}$=0. In this case, the wind turbine supplies only the load demand. Case II shows I/V curve in a mode where $I_{ch\text{-}ref} > 0$. In this case, the battery controller tries to charge BESS until I_B=-$I_{ch\text{-}ref}$. This transfers the I/V curve to the left in comparison with Case I, extending the length of the flat or smooth section of the curve from $I_{B\text{-}max}$ to ($I_{B\text{-}max}$+$I_{ch\text{-}ref}$). In other words, the WTG in Case II spends a portion of its power on supplying the load demand while another portion of power is spent on charging the battery. In this case, if the total load demand and reference battery charge current ($I_{ch\text{-}ref}$) exceed the WTG maximum production, then the battery will independently reduce the reference charging current, enabling the WTG to supply both the load current and battery charging current in a reduced level (I_{ch}<$I_{ch\text{-}ref}$). The above desired output is realized by relying on the battery's I/V characteristic curve independently without the need for an external reference or any centralized management system.

In this segment the target is to analyze the impact of load increasing on the characteristic curve in Figure 9. According to Figure 10, the load current is initially at point A, where the WTG charges the battery with the current of $I_{ch\text{-}ref}$ and supplies the total load demand.

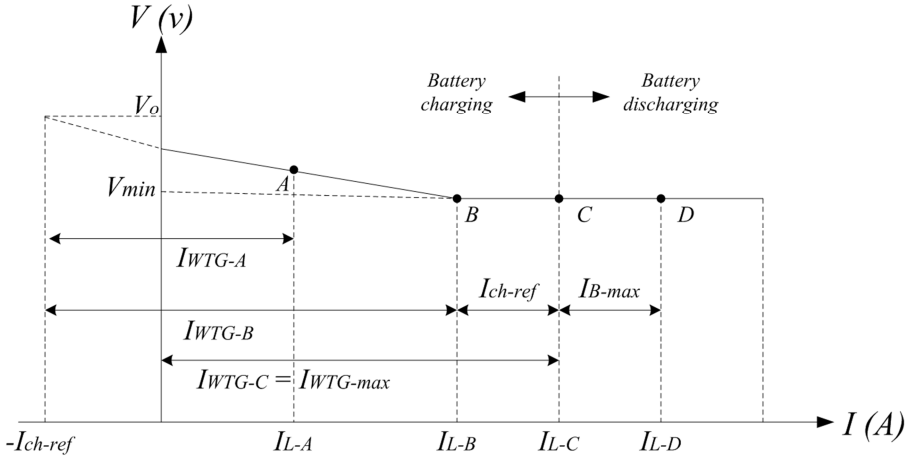

Figure 10. *Equivalent I/V characteristics curve of WTG and battery with increasing load trajectory.*

The WTG supplies any load increase until point B, where the wind turbine reaches its maximum nominal power ($I_{WTG\text{-}max}$) at voltage V=V_{min}, while supplying the load demand and battery charge current reference simultaneously. If the load current exceeds point B, the WTG will attempt to reduce the voltage to below V_{min} according to its droop characteristic. Hence, the battery begins to regulate the voltage within V_{min} by its PI controller. In this case, since the output current of wind turbine has reached its maximum value, any increase in the load demand will curtail the current flow to charge the battery. As a result, the battery regulates voltage as a controlled power source. In other words, the WTG regulates its output current within the nominal value, acting as a controlled power source. If the load current increases to point C, the battery charge current in this case becomes zero and the total output current of wind turbine will be spent on supplying load demand. If the load current exceeds point C and reaches to point D, the battery begins to discharge so as to supply the increased portion of load over the maximum current of the wind turbines. In this case, the battery controls and stabilizes the voltage as a constant voltage source in the flat part of I/V curve. Figure 11 illustrates the block diagram of battery control strategy.

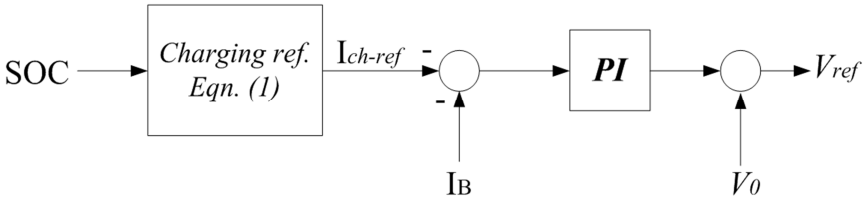

Figure 11. *Control diagram of battery system.*

The control system is applied to the battery converter in order to achieve I/V characteristic curve in accordance with the above diagram. In order to regulate the DC link voltage within the nominal value, the battery DC-DC converter is controlled by a PI controller with internal current control loop.

6. Decentralized Coordination of PV, WTG and Battery

The combination of characteristic curves PV, WTG and battery forms a multi-segment I/V characteristic curve

reflecting the decentralized synchronization of entire DC microgrid according to Figure 12.

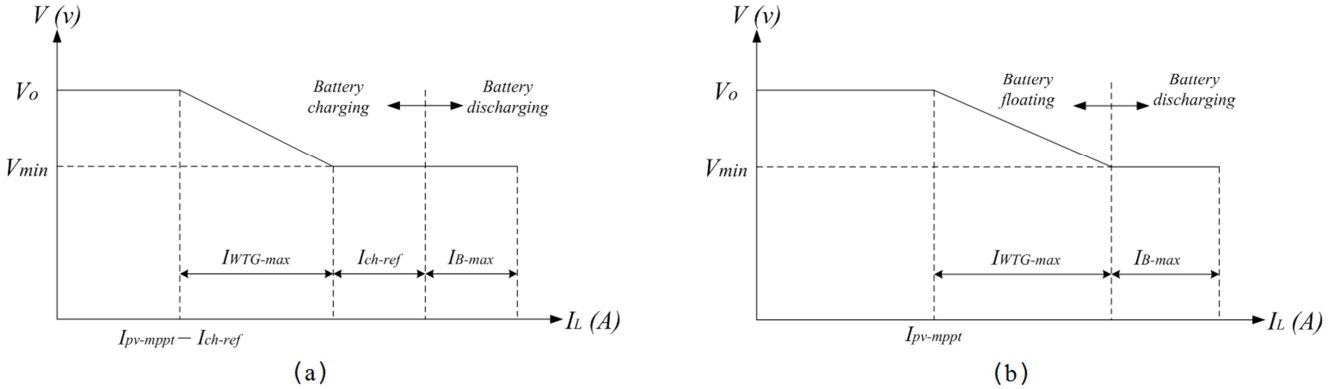

Figure 12. *Multi-segment characteristics of DC microgrid: (a) When $I_{ch-ref}>0$, (b) When $I_{ch-ref}=0$.*

The left side of the I/V curve in Figure 12 (a) depicts the DC microgrid operation area in which the PV module act as a voltage source with constant power delivering based on the MPPT, whereas the WTG and battery act as controlled power sources. In this section, the PV module regulates voltage by supplying the load demand and supporting the power balance within the microgrid. In the flat part of the curve on the left, the battery functions as a voltage source with constant voltage to supply the peak load demand in the microgrid. In this section, the microgrid voltage is regulated by the battery, while PV module and WTG serve as controlled power sources. In the middle section of the curve, (droop), the PV module and battery act as controlled power sources, while the WTG regulates the microgrid voltage based on its droop characteristic. It should be noted in Figure 12 (a), $I_{PV-MPPT}$ has been assumed to be greater than I_{ch-ref}. When $I_{PV-MPPT}$ is smaller than I_{ch-ref} or equal to zero, the behavior of microgrid characteristic curve will be according to Figure 9. When the battery is fully charged (I_{ch-ref}=0), the curve in Figure 12 (a) is transferred to the right forming the curve in Figure 12 (b). As a result, all operating modes described in the previous section will hold true for all the DC microgrid units for the curve in Figure 12 (b).

7. Simulation Results

A DC microgrid composed of distributed generation units of PV and WTG and battery energy storage system was simulated within MATLAB/SIMULINK so as to evaluate the performance of the proposed control strategy. Table 1 displays the microgrid parameters. Performance of the proposed strategy was assessed through several operational scenarios and altering the dc power load as well as the solar radiation level. In the first scenario, the performance of DC microgrid control strategy was evaluated in response to 8 kW of load. Then, the microgrid behavior was analyzed in 12 kW of load and in the third scenario; the microgrid performance and unit outputs were assessed by altering the solar radiation levels.

Table 1. *DC microgrid parameters.*

Parameter	Symbol	Value
DC bus voltage Ref.	V_{dc-ref}	250 V
Maximum PV power	P_{pv-max}	10 KW
Maximum WTG power	$P_{WTG-max}$	4 KW
Nominal virtual resistance	R_d	0.8 Ω
Low voltage threshold	V_L	230 V
High voltage threshold	V_H	260 V
Nominal battery capacity	C_{bat}	40 A.h
Initial SOC of battery	SOC	65%
Minimum value of SOC	SOC_{min}	40%
Maximum value of SOC	SOC_{max}	80%

Figure 13 shows the voltage/power curve of PV module. According to this graph, the PV arrays can generate and deliver maximum power of 10 kW at 1000 watts per square meter (w/m^2) of radiation level at 55 V. The red circles on the curve represent the maximum power point (MPP) traced and generated by the MPPT algorithm.

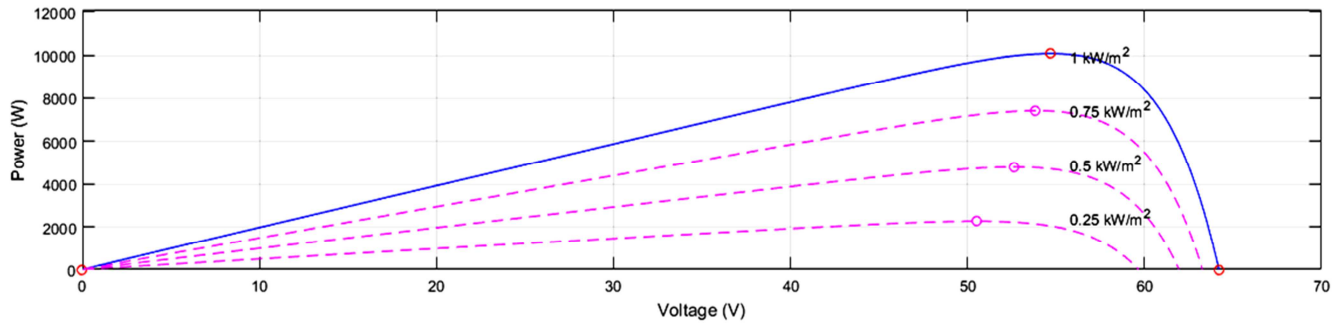

Figure 13. *Voltage/Power characteristic of PV module in 25°C and different radiation levels.*

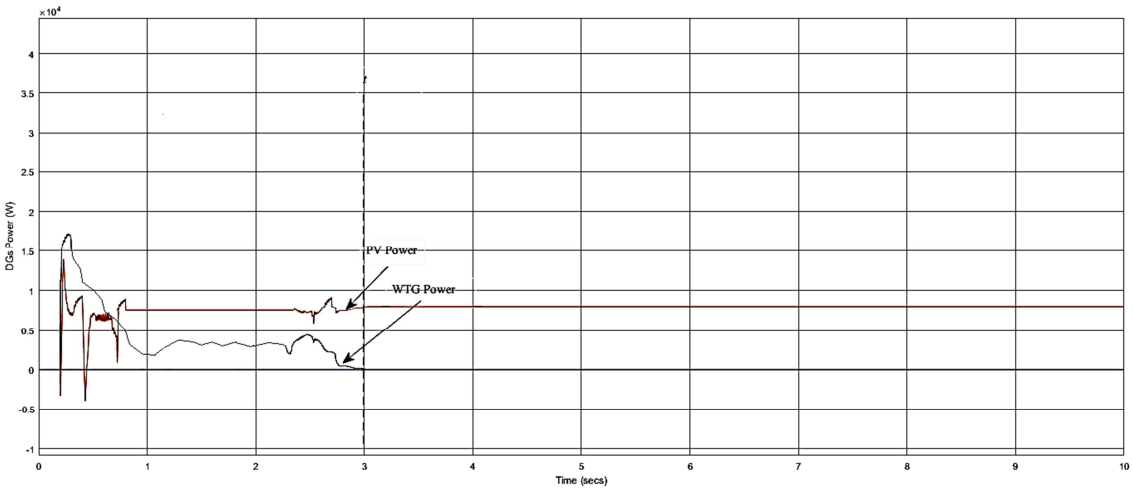

(a)

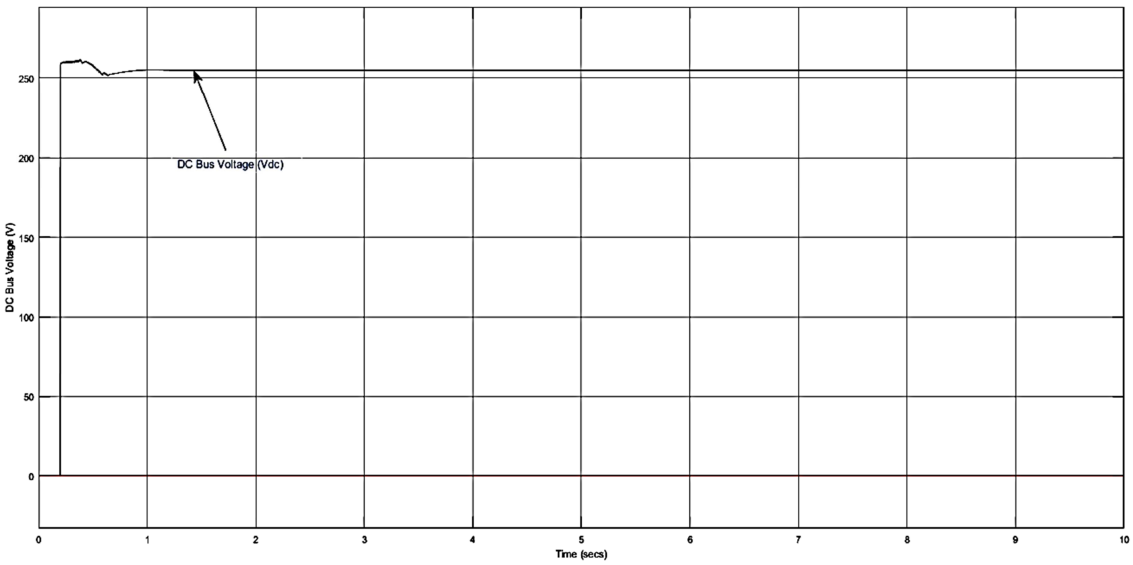

(b)

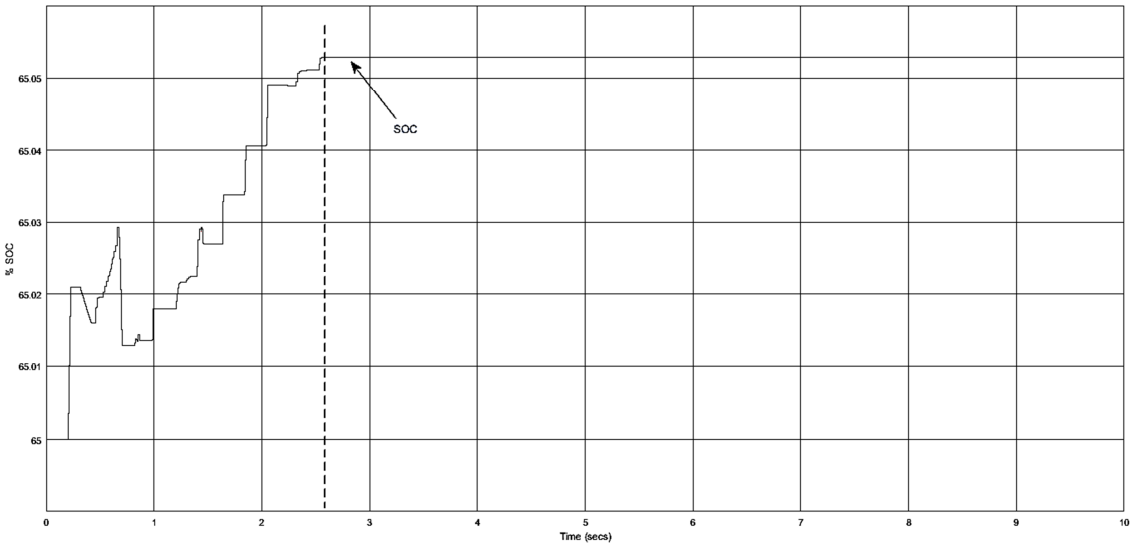

(c)

Figure 14. *Simulation results in 8 KW constant power load: (a) Power generation of DGs, (b) DC bus voltage, (c) Battery SOC.*

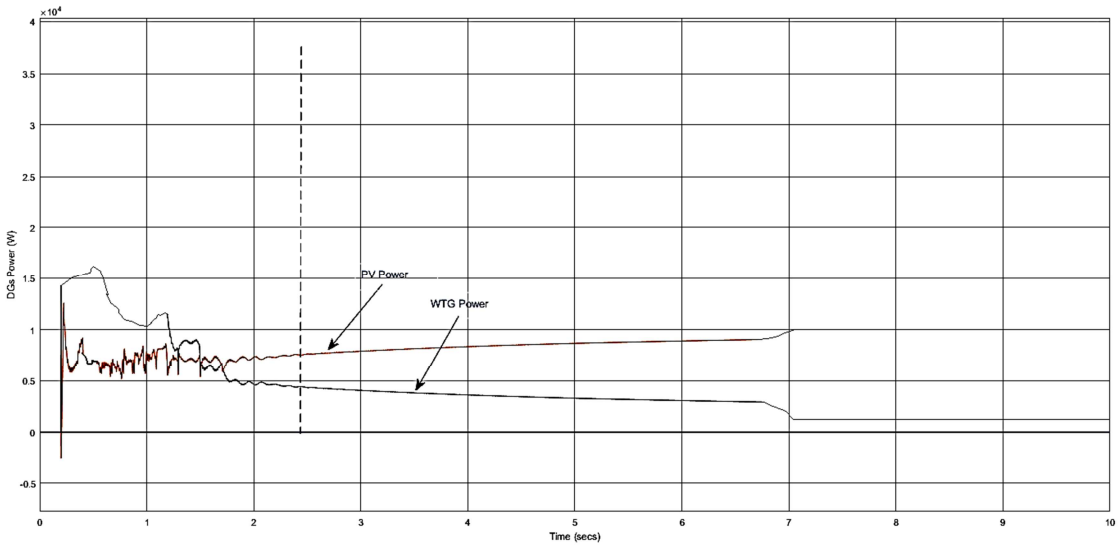

(a)

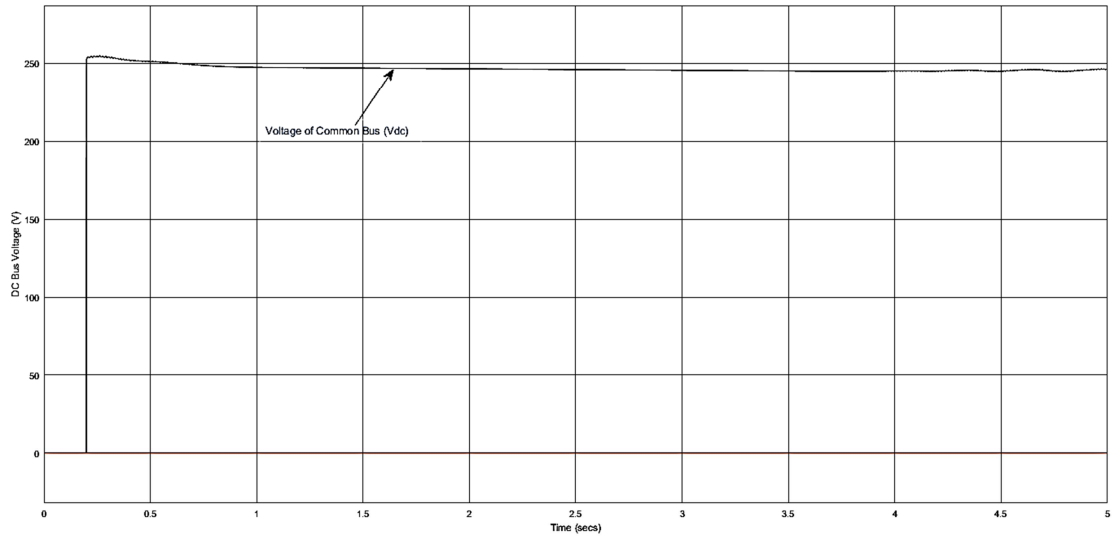

(b)

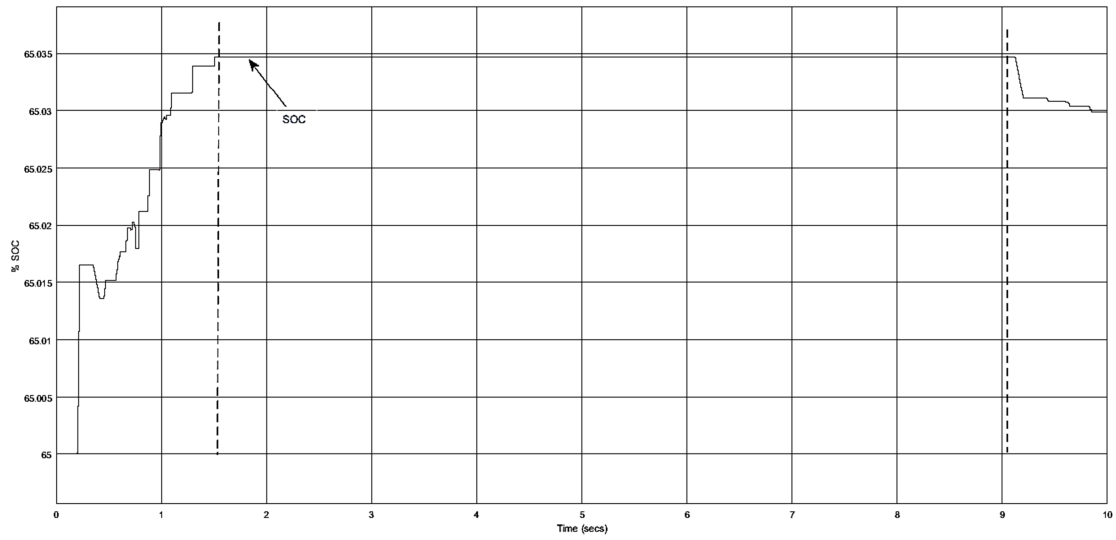

(c)

Figure 15. *Simulation results in 12 KW constant power load: (a) Power generation of DGs, (b) DC bus voltage, (c) Battery SOC.*

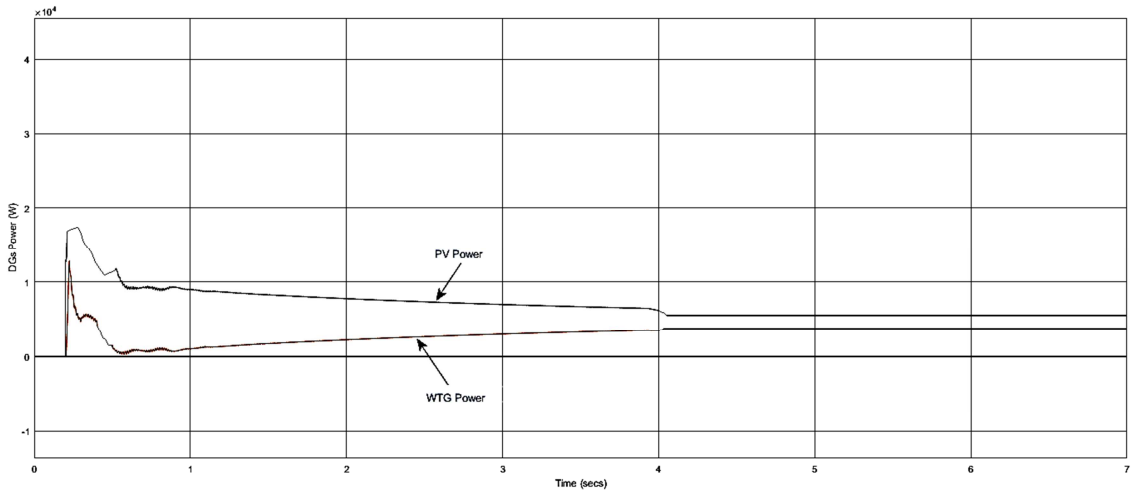

(a)

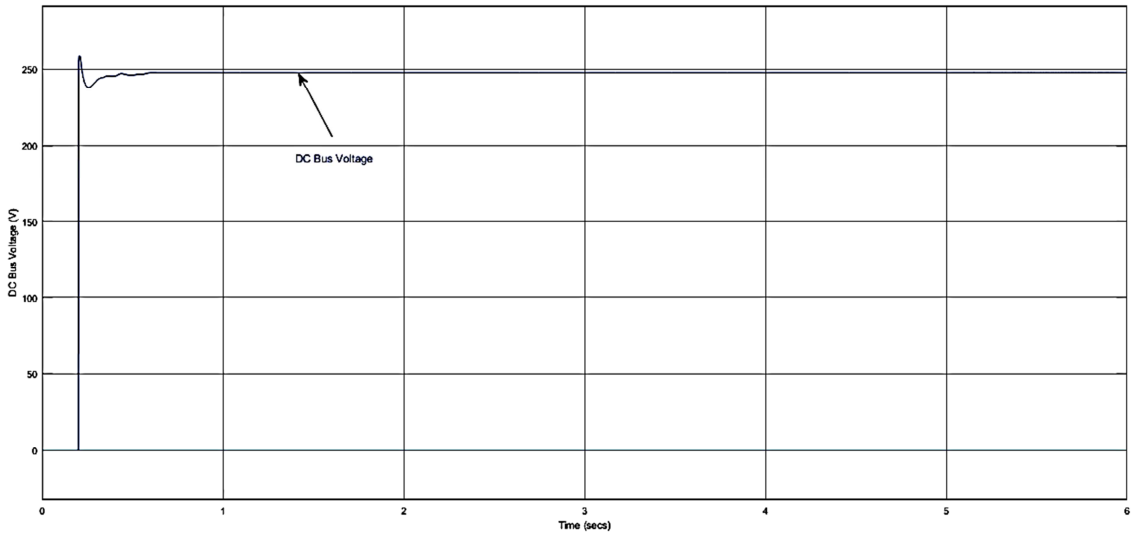

(b)

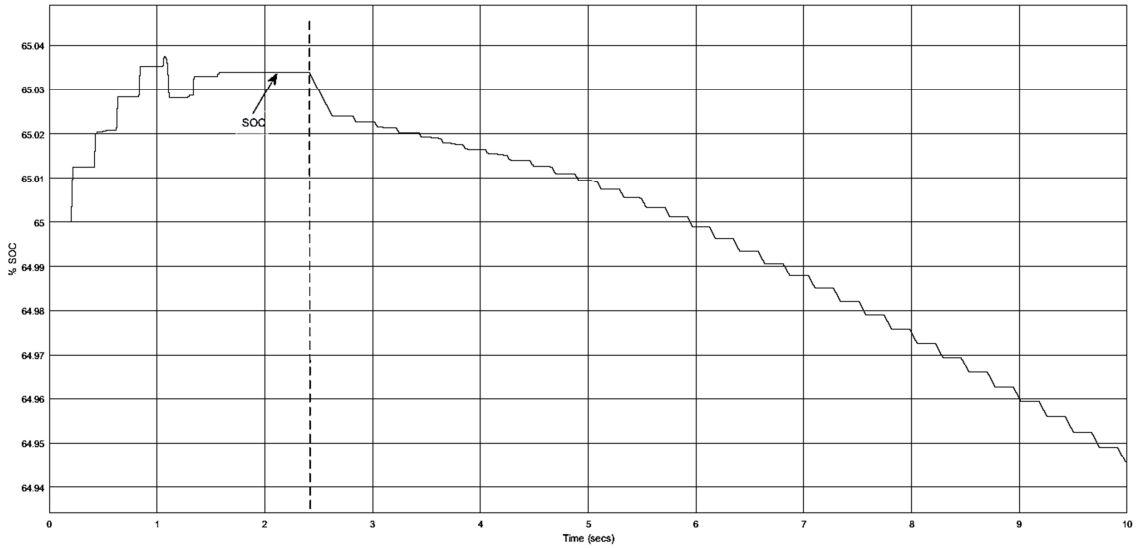

(c)

Figure 16. *DC microgrid performance in 10 KW constant power load and 500 w/m^2 radiation: (a) Power generation of DGs, (b) DC bus voltage, (c) Battery SOC.*

This study involved the MPPT algorithm based on conventional Perturb & Observe method to extract the maximum power of PV arrays. According to this algorithm, it can be shown that dP/dV becomes zero at the maximum power point, before which the value of power becomes positive and then negative. According to the above algorithm, if dP/dV is positive, the algorithm progresses on the voltage/power curve by increasing the voltage until it reaches dP/dV=0. If dP/dV is negative, the algorithm moves in the opposite direction to the point where the voltage/power variations are zero, introducing that as maximum power point.

Figure 14 illustrates the results of DC microgrid behavior under fixed power load of 8 kW. According to Figure 14 (a) the DGs transients run on in the beginning of the simulation and after t=3s, DGs reach their stable output. Since the maximum power of PV array is 10 kW based on the MPPT algorithm, where the load demand is lower than the maximum production of the module, the operating point will transfer the PV out of the MPP region, adapting the power generation to the load demand. Otherwise, the excess power generated by PV array will increase the common bus voltage beyond the allowable range. Therefore, the PV array in this scenario adapts its output to the load power as the output of wind turbine generator (WTG) will be zero through droop control. In this case, the PV array will act as a voltage source in the microgrid, adapting its output to the load demand. Moreover, the battery does not charge in this mode since the battery SOC is maintained within the range of 40 to 80% in order to prevent full drain and extend the life of capacitors (battery has initial SOC of 65%) as the PV controller supplies only load demand by regulating the operating point. Figure 14 (b) displays the DC link voltage variations under constant power load of 8 kW. Since the nominal voltage of microgrid was set to be 250 V, the common bus voltage is established on 254 volts after the initial transients. The voltage stabilizes on a value greater than the operating voltage because the load demand is lower than the PV power generation. In other words, since the allowable range of DC bus voltage lies within 230 to 260 volts, the lower level of load demand than the MPPT power of PV arrays increase the common bus voltage amplitude to a value higher than the operating voltage. At this point, the PI controller of PV unit will be responsible for regulating and stabilizing the voltage by curtailing the generation power of the module. Figure 14 (c) shows the battery charge level (SOC). According to an overview of the problem and because the PV module adapts its output to supply load the entire load, the battery in this case is first slightly charged, and then remains in the floating status without any more charge and discharge process. In this case, since the DC bus voltage is within the allowable range, the PI controller output of the battery is zero and there is no charge and discharge status.

Figure 15 illustrates the results of DC microgrid performance under fixed power load of 12 kW. In Figure 15 (a) at the beginning and end of the resource dynamics, the MPPT algorithm of PV module is enabled due to increased load demand and after 6 seconds, it delivers to the network its nominal power equivalent to 10 kW as the WTG supplies the rest of load demand equivalent to 2 kW. Notably, since the controllers of PV and WTG are adjusted in perfect coordination with each other, the wind turbine will supply the power shortage based on its droop characteristic so long as the power output of PV module reaches its nominal value (10 kW). After stabilizing the power generation of PV in MPPT mode on 10 kW, wind turbine reduces its output to 2 kW. Figure 15 (b) shows the DC common bus voltage variations. As shown, the DC link voltage with applying 12 kW of load begins to decrease to 250 volts of according to the droop characteristic of WTG. Since the WTG supplies the load demand equivalent to 2 kW lower than its nominal power, the DC link voltage is stabilized with a slight drop at 245 volts. Figure 15 (c) shows the battery charge level (SOC). In this case, since the power generation of DGs is based on load demand, there is no significant changes in the battery charge level and battery SOC remains on 65% of the initial value in floating mode. Before the microgrid reaches its steady state at t=7s, however, a portion of the excess power available in the battery is absorbed, increasing the battery SOC. After this point, since the power generation of DGs matches the load demand, the excess power will not be generated by the sources, leaving the battery in floating mode. Furthermore, the PI controller output of battery is zero without any charge and discharge status, since the battery SOC is within the specified range.

Figure 16 illustrates the results of DC microgrid performance by reducing the level of solar radiation from 1000 w/m^2 to 500 w/m^2. In this scenario, the generation power of PV is halved according to the voltage/power characteristic curve shown in Figure 13. In the MPPT mode, the output power will be maximum 5 kW. In this scenario, the dc constant power load of 10 kW is applied on the microgrid. Figure 15 (a) displays the production capacity of the hybrid unit and WTG. PV module supplies 5 kW of 10 KW load power after the system transients running on according to the radiation levels. Meanwhile, the wind turbine generator delivers its maximum power in order to supply constant power load at t=4s. In this mode, according to the droop characteristic of the wind turbine, the common bus voltage will begin to decrease. As the voltage value reaches the lower limit of the allowed range (230 V), the PI controller is activated to discharge the battery system and reducing the battery SOC, so as to regulate and maintain the voltage value within the allowable range. In this situation, the PV module behaves similar to a controlled power source according to the control system in the microgrid, delivering maximum power of PV array. Since the DGs production capacity in this scenario are 9 kW, the remaining one kW of power should be supplied by the battery through curtailing the SOC. As a result, the battery is slightly charged during the microgrid transients, followed by discharging and curtailing the SOC so as to supply the one kW of load demand shortage. It is noteworthy this situation could

continue until the battery SOC level reaches its lowest threshold of 40%, in which case the battery discharge status is disabled and the battery will be in charge or floating status. If in this case the total generation power of DGs is lower than the load demand, the load shedding scenario should be implemented which is outside the scope of this study. Figure 16 (b) displays the range of common bus voltage variations. As described in Section (a), the common bus voltage drops as the wind turbine supplies a portion of the load demand according to its droop characteristic. Hence, the battery system controller injects I_B into the DC link and supplying 1 kW power shortage to stabilize the limitation of V_{dc} on 242 volts. Moreover, Figure 16 (c) shows the SOC level of the battery system. The battery will start discharging to supply the shortage of load demand. In other words, after delivering of 9 kW by the PV and wind turbine, the battery system will supply the rest of load demand. Reduced level of battery SOC continues to minimum value of 40%, at which point it goes to floating status according to the scenario defined for the for battery based on the generation power of the DGs. Notably, the allowable range of 40 to 80 percent was assigned for the battery SOC in order to avoid full discharge of capacitors and extend the life of the BESS.

8. Conclusions

This paper proposed a new decentralized power management strategy for a DC microgrid controlled through droop method based on the adaptive I/V characteristic curve for DGs and battery energy storage system. The proposed control strategy was applied locally and without dependency on telecommunication links or any centralized energy management system on each of the distributed generation units and battery in real-time. The newly proposed decentralized technique can regulate the generation of PV module based on the MPPT algorithm or the power output of WTG based on its droop characteristic, so as to supply the load demand or recharge the battery. In fact, the proposed I/V characteristic for the battery is regulated locally and in real-time. The outcome is that power can be injected into the DC microgrid when the load has exceeded the total generation capacity of DGs. Moreover, the battery is integrated into the microgrid either in charge or floating modes based on the SOC and the conditions of generation and consumption. The newly proposed control scheme can add to the microgrid any number of distributed generation units or batteries without violating or interfering with the generalities offered. Hence, the proposed strategy can enhance the efficiency and flexibility of DC microgrids. The proposed decentralized control scheme was evaluated and validated through simulation in MATLAB/SIMULINK.

References

[1] F. Blaabjerg, Z. Chen, S. Kjaer, "Power electronics as efficient interface in dispersed power generation system", *IEEE Trans. Power Electron*, vol. 19, no. 5, pp. 1184-1194, 2004.

[2] F. Blaabjerg, R. Teodorescu, M. Lisserre, A. Timbus, "Overview of control and grid synchronization for distributed power generation systems", *IEEE Trans. Ind. Electron.*, vol. 53, no. 5, pp. 1398-1409, 2006.

[3] M. Saeedifard, M. Graovac, R. Dias, R. Iravani, "DC power systems, challenges and opportunities", *in Proc. IEEE Power Energy Soc. Gen. Meeting*, Minneapolis, MN, USA, July 2010, pp. 1-7.

[4] B. Patterson, "DC come home: DC microgrids and the birth of the Enernet", *IEEE Power Energy Mag.*, vol. 10, no. 6, pp. 60-69, 2012.

[5] Canadian Energy Efficiency Alliance, "Demand side management framework for Ontario", *www.iea.org*, Feb. 2004.

[6] A. Kahrobaeian, Y. Ibrahim Mohamed, "Network-Based hybrid distributed power sharing and control for islanded microgrid systems", *IEEE Trans. Power Electron.*, vol. 30, issue 2, pp. 603-617, 2015.

[7] S. Anand, B. Fernandes, M. Guerrero, "Disstributed control to ensure proportional load sharing and improve voltage regulation in low voltage DC microgrids", *IEEE Trans. Power Electron.*, vol. 28, issue 4, pp. 1900-1913, 2013.

[8] Z. Zeng, H. Yang, S. Tang, R. Zhao, "Objective-Oriented power quality compensation of multifunctional grid-tied inverters and its application in microgrids", *IEEE Trans. Power Electron.*, vol. 30, issue 3, pp. 1255-1265, 2015.

[9] Wei Du, Q. Jiang, M. Erikson, R. Lasseter, "Voltage-Source control of PV inverter in a CERTS microgrid", *IEEE Trans. Power Delivery*, vol. 29, issue 4, pp. 1726-1734, 2014.

[10] A. Dimeas, N. Hatziargyriou, "Operation of a multiagent system for microgrid control", *IEEE Trans. Power Systems*, vol. 20, issue 3, pp. 1447-1455, 2005.

[11] Liang Che, M. Shahidehpour, "DC microgrids: Economic operation and enhancement of resilience by hierarchical control", *IEEE Trans. Smart Grid*, vol. 5, issue 5, pp. 2517-2526, 2014.

[12] J. M. Guerrero, J. C. Vasquez, J. Matas, M. Castilla, L. G. D. Vicuna, "Hierarchical control of droop-controlled AC and DC microgrids- A general approach to standardization", *IEEE Trans. Ind. Electron.*, Vol. 58, Issue 1, pp. 158-172, 2011.

[13] R. Majumder, "A hybrid microgrid with DC connection at back to back converters", *IEEE Trans. Smart Grid*, vol. 5, issue 1, pp. 251-259, 2014.

[14] B. Wang, M. Sechilariu, F. Locment, "Intelligent DC microgrid with smart grid communications: Control strategy consideration and design", IEEE Trans. Smart Grid, vol. 3, no. 4, pp. 2148-2156, 2012.

[15] P. C. Loh, D. Li, Y. K. Chai, F. Blaabjerg, "Autonomous control of interlinking converter with energy storage in hybrid AC-DC microgrid", IEEE Trans. Industry Applications, vol. 49, issue 3, pp. 1374-1382, 2013.

[16] A. Bidram, A. Davoudi, "Hierarchical structure of microgrids control system", *IEEE Trans. Smart Grid*, vol. 3, no. 4, pp. 1963-1976, 2012.

[17] H. Dagdougui, R. Sacile, "Decentralized control of the power flows in a network of smart microgrids modeled as a team of cooperative agents", *IEEE Trans. Control Systems Technology*, vol. 22, issue 2, pp. 510-519, 2014.

[18] Lie Xu, Dong Chen, "Control and operation of DC microgrid with variable generation and energy storage", *IEEE Trans. Power Delivery*, vol. 26, no. 4, pp. 2513-2522, 2011.

[19] X. Lu, J. M. Guerrero, K. Sun, J. C. Vasquez, "An improved droop control method for DC microgrids based on low bandwidth communication with DC bus voltage restoration and enhanced current sharing accuracy", *IEEE Trans. Power Electronics*, vol. 29, no. 4, pp. 1800-1812, 2014.

[20] H. Kakigano, Y. Miura, T. Ise, "Low voltage bipolar type DC microgrid for super high quality distribution", *IEEE Trans. Power Electron*., vol. 25, pp. 3066-3075, 2010.

[21] Liang Che, Mohammad Shahidehpour, "DC microgrids: Economic operation and enhancement of resilience by hierarchical control", *IEEE Trans. Smart Grid*, vol. 5, issue 5, pp. 2517-2526, 2014.

[22] M. B. Camara, B. Dakyo, H. Gualous, "Polynomial control method of DC-DC converters for DC bus voltage and currents management battery and super-capacitors", *IEEE Trans. Power Electron*., vol. 27, no. 3, pp. 1455-1467, 2012.

[23] N. L. Diaz, T. Dragicevic, J. C. Vasquez, J. M. Guerrero, "Intelligent distributed generation and storage units for DC microgrids- A new concept on cooperative control without communications beyond droop control", *IEEE Trans. Smart Grid*, vol. 5, issue 5, pp. 2476-2485, 2014.

[24] Y. K. Chen, Y. Wu, C. Song, Y. S. Chen, "Design implementation of energy management system with fuzzy control for DC microgrid systems", *IEEE Trans. Power Electronics*, vol. 28, no. 4, pp. 1563-1569, 2013.

[25] T. Dragicevic, J. M. Guerrero, J. C. Vasquez, D. Skrlec, "Supervisory control of an adaptive-droop regulated DC microgrid with battery management capability", *IEEE Trans. Power Electronics*, vol. 29, issue 2, pp. 695-706, 2014.

[26] K. Strunz, E. Abbasi, D. N. Huu, "DC microgrid for wind and solar integration", IEEE Journal of Emerging and Selected Topics in Power Electronics, vol. 2, no. 1, pp. 115-126, 2014.

[27] K. Sun, L. Zhang, Y. Xing, J. M. Guerrero, "A distributed control strategy based on DC bus signaling for modular photovoltaic generation systems with battery energy storage", *IEEE Trans. Power Electron*., vol. 26, pp. 3032-3045, 2011.

[28] R. S. Balog, P. T. Krein, "Bus selection in multi-bus DC microgrids", *IEEE Trans. Power Electron*., vol. 26, pp. 860-867, 2011.

[29] R. Simanjorang, H. Yamaghuchi, H, Ohashi, K. Nakao, T. Ninomiya, S. Abe, M. Kaga, A. Fukui, "High efficiency high power DC-DC converter for energy and space saving of power supply system in a data center", *in Proc. Appl. Power Electron., Conf*., 2011, pp. 600-605.

[30] Z. Miao, L. Xu, V. R. Disfani, L. Fam, "An SOC-based battery management system for microgrids", *IEEE Trans. Smart Grid*, vol. 5, no. 2, pp. 966-973, 2014.

[31] Y. Cao, S. Tang, C. Li, P. Zhang, Y. Tan, Z. Zhang, J. Li, "An optimized EV charging model considering tou price and SOC curve", *IEEE Trans. Smart Grid*, vol. 3, no. 1, pp. 388-393, 2012.

[32] P. Thounthong, S. Rael, B. Davat, "Control algorithm of fuel cell and batteries for distributed generation system", *IEEE Trans. Energy Convers*., vol. 23. no. 1, pp. 148-155, 2008.

[33] R. F. Nelson, "Power requirements for batteries in hybrid electric vehicles", *Journal of Power Sources*, vol. 91, no. 1, pp. 2-26, 2000.

[34] E. Koutroulis, K. Kalaitzakis, "Novel battery charging regulation system for photovoltaic applications", *IEE Proc. Electr. Power Appl*., vol. 151, no. 2, pp. 191-197, 2004.